Journal of Applied Fluid Mechanics, Vol. 11, No. 5, pp. 1377-1386, 2018.
Available online at www.jafmonline.net, ISSN 1735-3572, EISSN 1735-3645.
DOI: 10.29252/jafm.11.05.28814

Experimental and Theoretical Study on Spray Angles of Bi-Swirl Coaxial Injectors

W. Yoon and K. Ahn†

[1] *School of Mechanical Engineering, Chungbuk National University, Chungdae-ro 1, Seowon-gu, Cheongju, Chungbuk 28644, Korea*

†*Corresponding Author Email: kbahn@cbnu.ac.kr*

(Received January 23, 2018; accepted April 29, 2018)

ABSTRACT

An experimental and theoretical study was undertaken to investigate the effects of the recess length, swirl direction, and mixture ratio on the spray angles of the bi-swirl coaxial injectors with the inner, closed-type and outer, open-type swirl injectors. Eight bi-swirl coaxial injectors with a range of recess lengths and different swirl directions between the inner and outer swirl injectors were used. As the recess length was increased, each bi-swirl coaxial injector exhibited external-mixing, tip-mixing, or internal-mixing spray characteristics. To measure the spray angles, cold-flow tests for which the mass flow rates of the two injectors were varied were performed to capture the spray images. The single-injection results indicated that the spray cone angles of both the inner and outer swirl injectors were relatively unaffected by the mass flow rate and the swirl direction, with the recess length influencing the spray cone angles of the inner swirl injectors. The bi-injection tests show that the spray angles are significantly dependent on the recess length and the mixture ratio, while also being affected by the swirl direction, especially regarding the internal-mixing bi-swirl coaxial injectors. Theoretical models that can predict the spray angles were developed and compared using the experimental data. The theoretical models could approximate the combined spray angles of the internal-mixing bi-swirl coaxial injectors.

Keywords: Bi-swirl coaxial injector; Spray angle; Recess length; Swirl direction; Mixture ratio.

NOMENCLATURE

A	area
COS	co-swirl
CTS	counter-swirl
d	diameter
K	swirl injector geometric constant
l	length
MR	ratio of the inner mass flow rate to the outer mass flow rate
m	mass flow rate
n	number of tangential holes
R	radial distance from the injector's center to the tangential hole's center
RN	Recess number
r	radius
U	axial velocity
V	circumferential velocity
W	radial velocity
ΔP	injection pressure differential, bar
θ	spray cone half angle
ρ	flow density
φ	filling coefficient

SUBSCRIPTS

c	collision point of the inner liquid sheet on the outer nozzle wall
em	external mixing
i	supplied from the inner swirl injector
im	internal mixing
in	inner swirl injector nozzle
ine	inner swirl injector nozzle exit
h	tangential hole
gc	gas core
ma	mass-averaged radial location
n	nozzle
nw	nozzle wall
ne	nozzle exit
o	supplied from the outer swirl injector
on	outer swirl injector nozzle
one	outer swirl injector nozzle exit
R	recess
s	swirl chamber
t	totally combined liquid

1. INTRODUCTION

Swirl injectors have been applied to combustion devices such as liquid rocket engines, gas turbine engines, and internal combustion engines. Swirl injectors with tangential ports can be classified by their geometry, as follows: closed-type, open-type, or swirl coaxial (Ahn *et al.* 2011). In addition, the swirl coaxial injector can be further divided into gas-liquid swirl coaxial injectors and liquid-liquid bi-swirl coaxial injectors (Ahn *et al.* 2012; Jeon *et al.* 2011; Long 2004; Yang *et al.* 2008). The bi-swirl coaxial injector, which structurally consists of two swirl injectors, has been widely used with the liquid rocket engines to simultaneously discharge the liquid-phase fuel and oxidizer (Ahn *et al.* 2014; Gill and Nurick 1976).

The spray characteristics of swirl injectors, which are expressed by the spray cone angle, discharge coefficient, film thickness, breakup length, and droplet size/velocity, are influenced by the injector geometry and flow conditions. Experimental and numerical studies have been performed on both the closed-type and open-type swirl injectors over a long time period. Bayvel and Orzechowski (1993), Bazarov *et al.* (2004), Borodin *et al.* (2004), and Khavkin (2004) introduced theoretical methods to calculate the discharge coefficient, film thickness, and spray cone angle. Using abundant experimental data, they also proposed empirical equations for the swirl injectors. By investigating the effects of ambient pressure on a closed-type swirl injector through a combined theoretical/numerical analysis, Chen and Yang (2014) suggested a semi-empirical model for the prediction of the liquid-sheet shape. Vijay *et al.* (2015) reviewed the internal and external flow characteristics of the closed-type swirl injectors. Fu *et al.* (2010, 2011a,b, 2012) performed diverse research on the open-type swirl injectors, and proposed empirical equations for the film thickness, discharge coefficient, spray cone angle, and breakup length. From the cold-flow tests of numerous closed-type and open-type swirl injectors, Ahn and Choi (2017a,b) presented simple empirical equations for the prediction of the discharge coefficient of the swirl injectors and compared them with the previous equations.

Studies on the bi-swirl coaxial injectors have been carried out under both the cold-flow and hot-firing conditions. Sivakumar and Raghunandan (1998, 2003) investigated the droplet size and the merging characteristics of the liquid sheets. By performing the hot-firing tests, Ahn *et al.* (2011, 2012, 2014) and found that the recess length affected the discharge coefficient, combustion performance, combustion stability, and heat flux in a combustion chamber. As the recess length was increased, the combustion performance and heat flux increased, and the discharge coefficient and combustion stability sometimes decreased. Kim *et al.* (2003) showed the reduced spray angle of the merged liquid sheet in the bi-swirl coaxial injectors compared with the spray angles of the single-injection inner/outer liquid sheets, and it changed with the mixture ratio (MR). The spray characteristics of the bi-swirl coaxial injectors were extensively studied by Kim (2007) and Kim (2011). Kim (2007) used the bi-swirl coaxial injectors with the inner/outer closed-type swirl injectors, demonstrating the presence of three mixing conditions between the two liquids, as follow: external mixing, tip mixing, and internal mixing. It was reported that the spray angle, breakup length, mixing efficiency, and droplet size are affected by the recess length (mixing condition) and the MR. Kim (2011) extended the research of Kim (2007) in a study on the bi-swirl coaxial injectors with the inner closed-type and outer open-type swirl injectors. The liquid film thickness was investigated over a broad range of MRs, and it was shown that the film thickness changed with the varying of the recess length and the MR.

Since the spray angles of the bi-swirl coaxial injectors determine the propellant distribution and therefore the combustion zone, it is a critical design parameter of the combustion chamber. Although several in-depth studies have been completed, these are insufficient to gain a profound understanding and to predict the spray angles of the bi-swirl coaxial injectors. Therefore, the first objective of the present research is the systematic examination of the effects of the geometric and flow conditions that are found between the inner and outer swirl injectors on the spray angle of the bi-swirl coaxial injectors. The second objective is the development of theoretical models for the prediction of the spray angle. For these purposes, the elements of eight bi-swirl coaxial injectors with different recess lengths and swirl directions were manufactured, and cold-flow tests were carried out over a broad range of MRs.

2. EXPERIMENTAL METHODS

2.1 Bi-Swirl Coaxial Injectors and the Experimental Setup

A schematic of the bi-swirl coaxial injectors of the present study is shown in Fig. 1. The bi-swirl coaxial injectors comprise an inner closed-type swirl injector ($d_s > d_n$) and an outer open-type swirl injector ($d_s = d_n$). As shown in Fig. 1, the three parts were formed from stainless steel using the conventional computer numerical control (CNC) machining, and were welded into the element of each bi-swirl coaxial injector using the brazing technique (Yoon and Ahn 2017). Both the co-swirl and counter-swirl coaxial injectors were designed and manufactured. For all the bi-swirl coaxial injectors, the outer swirl injectors comprise the same geometry, and the swirl direction is clockwise in relation to the nozzle. The inner swirl injectors are the same, except for the nozzle length and the machining direction of the tangential holes. The inner swirl injector comprises eight tangential holes in two rows, and the outer injector comprises four holes in one row. The co-swirl coaxial injectors comprise the same swirl directions in the inner/outer swirl injectors and recess lengths of 0.0, 1.9, 3.6, 4.5, and 6.0 mm. On the contrary, the counter-swirl coaxial injectors comprise opposing swirl directions in the inner/outer injectors and recess lengths of 0.0, 3.6, and 6.0 mm. Here, the recess length is defined as

the distance between the inner injector nozzle tip and the outer injector nozzle tip.

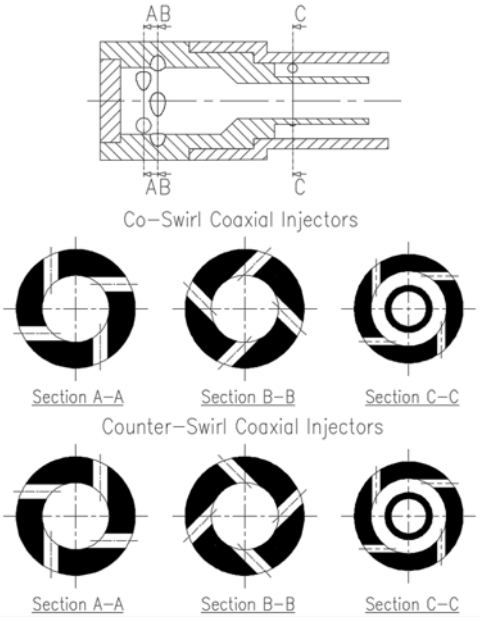

Fig. 1. Schematic of the present bi-swirl coaxial injectors.

Figure 2 shows the three mixing conditions for the bi-swirl coaxial injectors with respect to the recess length and their typical spray patterns. From the previous research (Ahn *et al.* 2011; Bazarov *et al.* 2004; Kim 2007), the mixing condition depends on the recess number (RN). The recess number is defined as the ratio of the recess length (l_R) to the distance between the inner injector nozzle tip and the collision point of the inner liquid sheet on the outer injector nozzle wall (l_c). When the RN is less than 1, the inner and outer liquid sheets do not mix inside the bi-swirl coaxial injector (external mixing). Near to the RN = 1, the inner liquid sheet collides with the outer liquid film around the outer injector nozzle tip, and thus the two liquid sheets interact partially inside the injector; this is known as tip, or intermediate, mixing. When the RN is higher than 1, the inner liquid sheet collides with the outer liquid film and the two liquids are mixed inside the injector (internal mixing). The recess numbers for the recess lengths of 0.0 mm, 1.9 mm, 3.6 mm, 4.5 mm, and 6.0 mm are 0.00, 0.53, 1.00, 1.25, and 1.66, respectively. The detailed geometric information regarding the bi-swirl coaxial injectors that were used in this study is summarized in Table 1.

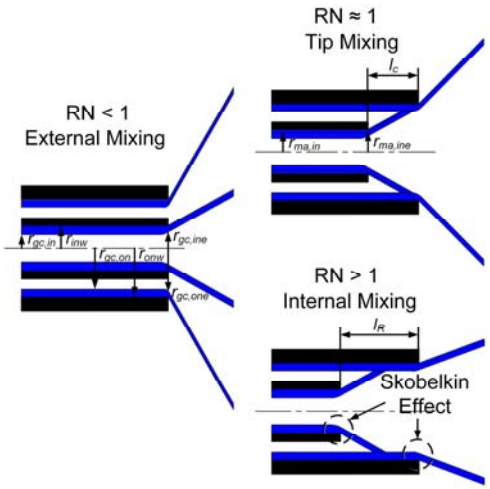

Fig. 2. Mixing conditions for the bi-swirl coaxial injectors and their spray patterns.

A schematic of the present experimental setup is illustrated in Fig. 3. Tap water was used as the liquid simulant instead of real propellants. The water in the tank, which was pressurized by a regulator connected to a compressed air bottle, was supplied and controlled by needle valves into each manifold of the bi-swirl coaxial injectors. The turbine flow meter (Kometer, NK-250) and a K-type thermocouple were installed in each supply line to measure the mass flow rate, and the pressure transducer (Sensys, PSH model) was located in each manifold to directly gauge the injection pressure. The detected data from these sensors were recorded by the NI Compact-DAQ system. The spray angles were obtained from back-lit spray images, which were taken using the high-speed camera (Vision Research, Phantom v9.1) and the light source (Polarion, PS-X1). For each test condition, 100 photographs were taken with an exposure time of 5 μs at 1000 fps. The spray angles

Table 1 Geometric information for the present bi-swirl coaxial injectors

Injector	Unit	Inner closed-type		Outer open-type		
K		0.98		16.48		
n_h	mm	8		4		
d_h		1.48		0.86		
d_s		6.7		7.5		
d_n		3.5		7.5		
R		2.45		3.25		
Swirl direction (COS)		Clockwise		Clockwise		
Swirl direction (CTS)		Counter-clockwise		Clockwise		
		Recess length				
COS coaxial injectors	mm	0.0	1.9	3.6	4.5	6.0
CTS coaxial injectors		0.0		3.6		6.0
		Recess number				
COS coaxial injectors		0.00	0.53	1.00	1.25	1.66
CTS coaxial injectors		0.00		1.00		1.66

were calculated using an image processing method that searched for the spray image edges.

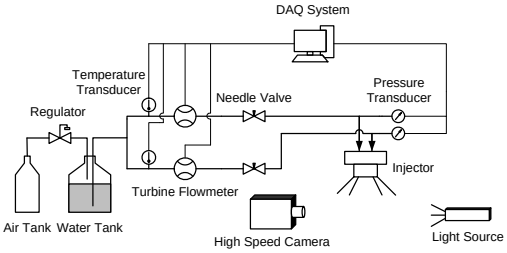

Fig. 3. Experimental setup for the cold-flow tests of the bi-swirl coaxial injectors.

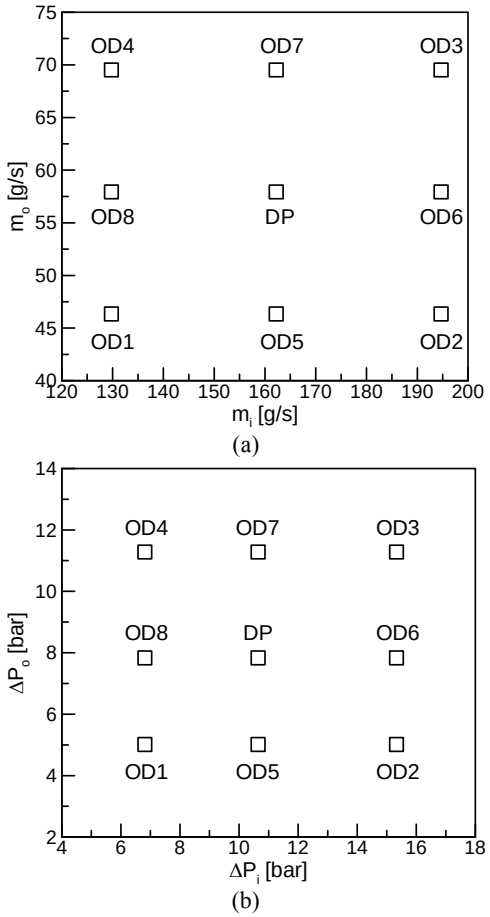

Fig. 4. Experimental conditions for the inner/outer mass flow rates (a) and their predicted injection pressure drops (b).

2.2 Experimental Conditions

Figure 4(a) shows the experimental conditions for the inner and outer mass flow rates. The injection pressure drops were predicted from the present injector dimensions and the previous empirical equations (Ahn and Choi 2017a,b), and they are plotted in Fig. 4(b). Here, DP is the nominal operating condition, and ODs are the off-nominal operating conditions with DP-based 20% deviations of the mass flow rate. Since the bi-swirl coaxial injector is designed for a liquid rocket engine thrust chamber, for which liquid oxygen is used through the inner swirl injector and the Jet A-1is used through the outer swirl injector, the inner mass flow rate is larger than that of the outer. The ratio of the inner mass flow rate to that of the outer (MR) is varied from 1.87 to 4.20. Further details of the experimental conditions are summarized in Table 2.

3. THEORETICAL ANALYSIS

3.1 Single-Injection Spray Cone Angle

From the previous research (Ahn and Choi 2017a,b; Bayvel and Orzechowski 1993; Kim 2013), the swirl injector geometric constant (K) is known to be the most important parameter affecting the spray angle for both the closed-type and open-type swirl injectors. If the spray of the swirl injector is fully developed under a sufficient injection pressure drop, its spray cone angle can be approximated as a function of the K. The swirl injector geometric constant is defined according to Eq. (1), and can be obtained using the geometric information of the swirl injector.

$$K = \frac{A_{nw}R}{A_h r_{nw}} = \frac{r_{nw}R}{nr_h^2} \tag{1}$$

The nozzle filling coefficient of the swirl injector is the ratio of the liquid film area to the nozzle area, and can be defined using Eq. (2). Assuming the principle of the maximum flow rate (Abramovich 1944), the filling coefficient can be expressed as a function of the K, as per Eq. (3).

$$\varphi_n = \frac{\pi(r_{nw}^2 - r_{gc,n}^2)}{\pi r_{nw}^2} \tag{2}$$

$$\frac{\sqrt{2}(1-\varphi_n)}{\varphi_n^{3/2}} = K \tag{3}$$

Due to the centrifugal force, the filling coefficient at the nozzle exit becomes smaller than that in the nozzle, thereby causing the radius of the gas core and the axial velocity to increase at the nozzle exit, as shown in Fig 2. This phenomenon is known as the Skobelkin effect. According to Bazarov *et al.* (2004), the filling coefficient at the nozzle exit is defined by, and can be obtained from, the filling coefficient in the nozzle, as follows:

$$\varphi_{ne} = \frac{\pi(r_{nw}^2 - r_{gc,ne}^2)}{\pi r_{nw}^2}, \varphi_{ne} = \frac{\varphi_n}{\sqrt{3-2\varphi_n}} \tag{4}$$

From the mass conservation, the axial velocities in the nozzle and at the nozzle exit can be expressed using Eq. (5). If the mass flow rate, density, area, and filling coefficient are known, one can calculate the axial velocities in the nozzle and at the nozzle exit.

Table 2 Detailed experimental conditions for the inner/outer mass flow rates

Test condition	DP	OD1	OD2	OD3	OD4	OD5	OD6	OD7	OD8
m_i [g/s]	162.21	129.77	194.65	194.65	129.77	162.21	194.65	162.21	129.77
m_o [g/s]	57.93	46.35	46.35	69.52	69.52	46.35	57.93	69.52	57.93
MR	2.80	2.80	4.20	2.80	1.87	3.50	3.36	2.33	2.24

$$m = \rho U_n \varphi_n A_n = \rho U_{ne} \varphi_{ne} A_n \quad (5)$$

The flow velocity in the tangential holes is obtained using Eq. (6). From the conservation of the angular momentum, the circumferential velocities at the nozzle wall, gas core, and mass-averaged radial location of the liquid film can be computed using Eq. (7).

$$V_h = \frac{m}{\rho n \pi r_h^2} \quad (6)$$

$$RV_h = r_{nw} V_{nw} = r_{gc,n} V_{gc,n} = r_{ma,n} V_{ma,n} = r_{ma,ne} V_{ma,ne}$$

$$r_{ma,n} = \sqrt{\frac{r_{gc,n}^2 + r_{nw}^2}{2}} = r_{nw} \sqrt{\frac{2-\varphi_n}{2}}$$

$$r_{ma,ne} = \sqrt{\frac{r_{gc,ne}^2 + r_{nw}^2}{2}} = r_{nw} \sqrt{\frac{2-\varphi_{ne}}{2}} \quad (7)$$

Based on the results of Eqs. (5) and (7), the spray cone half angle downstream of the swirl injector nozzle exit can be calculated using Eq. (8), for which the mass-averaged circumferential velocity at the radial location of the liquid film is applied. Using Eq. (8), it is possible to predict the spray cone half angle of the liquid sheets from the inner and outer swirl injectors of the bi-swirl coaxial injectors. The recess numbers in Table 1 were calculated using the spray cone angle that was obtained using Eq. (8), as follows:

$$\theta = tan^{-1}\left(\frac{V_{ma,ne}}{U_{ne}}\right) \quad (8)$$

When the recess length is so long that the liquid sheet from the inner swirl injector collides with the wall of the outer swirl injector, the spray angle will be changed. Assuming the axial momentum continuity (Eq. 9) and the mass continuity (Eq. 10), the filling coefficient of the liquid film on the outer swirl injector nozzle, which comes from the inner swirl injector, can be obtained. As with Eqs. (5-7), the spray half angle of the inner liquid sheet for the bi-swirl coaxial injector with the RN > 1 can be estimated as follows:

$$m_i U_{i,ine} = m_i U_{i,on} \quad (9)$$

$$m_i = \rho U_{i,on} \varphi_{i,on} A_{on} \quad (10)$$

$$\varphi_{i,one} = \frac{\varphi_{i,on}}{\sqrt{3-2\varphi_{i,on}}}, U_{i,one} = \frac{m_i}{\rho \varphi_{i,one} A_{on}}, V_{i,ma,one} = \frac{R_i V_{i,h}}{r_{i,ma,one}} \quad (11)$$

$$\theta_{i,one} = tan^{-1}\left(\frac{V_{i,ma,one}}{U_{i,one}}\right) \quad (12)$$

3.2 Bi-Injection Spray Angle

The spray angles from the bi-injection bi-swirl coaxial injectors should be calculated in consideration of the RN and the mixing conditions, such as the external mixing and the internal mixing. For the external-mixing bi-swirl coaxial injector, the previous researchers (Bazarov *et al.* 2004; Kim 2007) used Eqs. (13) and (14) to predict the spray angle of the combined liquid sheet, assuming the axial and circumferential momentum conservations; however, these equations assume that the two liquid sheets are totally combined outside the injector. Therefore, as with the present bi-swirl coaxial injectors, for two separate liquid sheets, these equations are not considered to be reasonable.

$$(m_i + m_o) U_{t,em} = m_i U_{i,ine} + m_o U_{o,one}$$

$$(m_i + m_o) V_{t,em} = m_i V_{i,ma,ine} + m_o V_{o,ma,one} \quad (13)$$

$$\theta_{t,em} = tan^{-1}\left(\frac{V_{t,em}}{U_{t,em}}\right) \quad (14)$$

For the internal-mixing bi-swirl coaxial injector, the following theoretical method is suggested. By assuming the continuity of the mass, axial, and circumferential momentums for the liquid sheet from the inner swirl injector nozzle exit and the liquid film from the outer swirl injector nozzle, the axial velocity, circumferential velocity, and filling coefficient of the combined liquid film on the outer swirl injector nozzle can be obtained according to Eqs. (15-17). As with Eq. (4), due to the Skobelkin effect, the axial velocity, circumferential velocity, and filling coefficient of the combined liquid film on the outer swirl injector nozzle exit can be calculated using Eq. (18). Therefore, the spray angle of the combined liquid sheet that discharges from the outer swirl injector nozzle exit can be predicted using Eq. (19).

$$(m_i + m_o) U_{t,on} = m_i U_{i,ine} + m_o U_{o,on} \quad (15)$$

$$m_i + m_o = \rho U_{t,on} \varphi_{t,on} A_{on} \quad (16)$$

$$(m_i + m_o) V_{t,ma,on} r_{t,ma,on} = m_i V_{i,ma,ine} r_{i,ma,ine} + m_o V_{o,ma,on} r_{o,ma,on} \quad (17)$$

$$\varphi_{t,one} = \frac{\varphi_{t,on}}{\sqrt{3-2\varphi_{t,on}}}, U_{t,one} = \frac{m_i + m_o}{\rho \varphi_{t,one} A_{on}}, V_{t,ma,one} = \frac{V_{t,ma,on} r_{t,ma,on}}{r_{t,ma,one}} \quad (18)$$

$$\theta_{t,im,one} = tan^{-1}\left(\frac{V_{t,ma,one}}{U_{t,one}}\right) \quad (19)$$

4. Experimental Results and Discussion

4.1 Single-Injection Spray Images and Spray Cone Angles

The spray patterns of the single-injection inner/outer swirl injectors for the co-swirl and counter-swirl coaxial injectors with the recess length of 0.0 mm are presented in Fig. 5 as a function of the injection pressure (i.e., the mass flow rate). Since the injection pressures above 4.5 bar were sufficiently high, all the spray patterns are fully developed, and the variation of the injection pressure only slightly affected the spray angles of both the inner and outer swirl injectors; although, the breakup lengths shortened with the increasing of the injection pressure. The swirl directions of the inner injectors in the co-swirl and counter-swirl coaxial injectors are opposing, but the corresponding influence on the spray angle is negligible.

Figure 6 shows the spray patterns of the single-injection inner swirl injectors at the DP condition for the co-swirl and counter-swirl coaxial injectors with respect to the recess length. Since the geometry

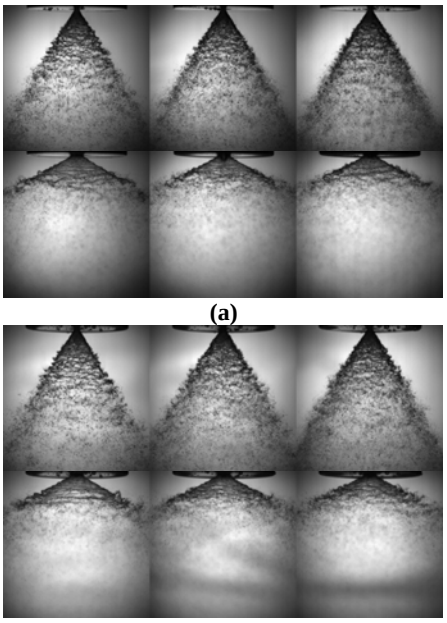

(a)

(b)

Fig. 5. Single-injection spray patterns with the variation of the mass flow rate for the co-swirl coaxial injector with the RN = 0.00 (a) and the counter-swirl coaxial injector with the RN = 0.00 (b) (from top to bottom: inner and outer swirl injectors; from left to right: OD1, DP, and OD3 conditions).

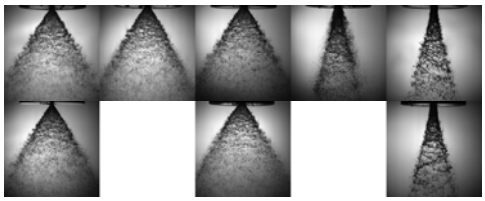

Fig. 6. Spray patterns of the single-injection inner swirl injectors at the DP condition with the varying recess length (from top to bottom: co-swirl and counter-swirl coaxial injectors; from left to right: RN = 0.00, 0.53, 1.00, 1.25, and 1.66).

of the outer swirl injectors for all the bi-swirl injectors is the same, the single-injection spray patterns do not exhibit any difference between the outer swirl injectors, and these are similar to those of Fig. 5. Although the co-swirl coaxial injectors comprise five recess lengths and the counter-swirl injectors comprise three recess lengths, it could be confirmed that the spray patterns of the inner swirl injectors depended on the recess number and the mixing characteristics. The spray patterns are similar except for the injectors with the RN > 1, which correspond to the internal mixing. When the RN > 1, the liquid sheet from the inner swirl injector collided with the outer injector nozzle wall, as shown in Fig. 2. From the conservation of angular momentum, the circumferential velocity reduced as the radius was increased, and this was expected based on Eq. (12). Further, this decreased the spray angle of the inner liquid sheet in the bi-swirl coaxial injectors with the RN > 1.

For the quantitative analysis, the spray angles of the single-injection inner and outer liquid sheets were measured from 100 photographs, and their averaged values are plotted in Fig. 7. To measure the spray angles, only the pre-breakup spray image was considered. For this purpose, the images from 10-15 mm downstream of the outer injector nozzle exit were cropped and binarized. By detecting and connecting the upper and lower edges of the cropped images, the spray cone angle was calculated. Since the liquid sheet is turbulent and fluctuated, the averaged value of the measured spray angles was used. The standard deviation of the measured spray angles is between 2° and 10°, depending on the test condition. The spray angles were predicted from the theoretical methods of Eqs. (8) and (12) using the geometric dimensions of the present bi-swirl coaxial injectors and the measured mass flow rates, and they are also presented in Fig. 7.

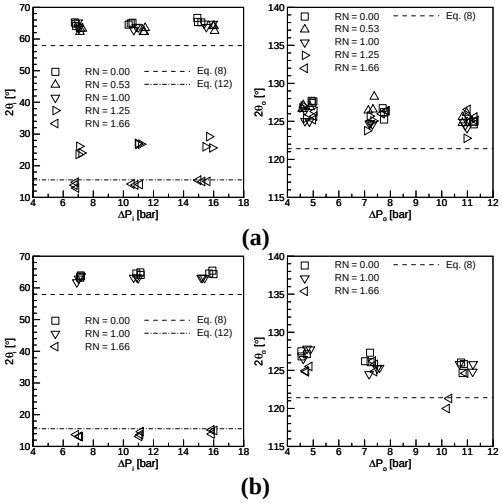

(a)

(b)

Fig. 7. Measured and calculated spray cone angles of the single-injection co-swirl coaxial injectors (a) and the counter-swirl coaxial injectors (b).

As could be anticipated from the spray images in Figs. 5 and 6, the spray angles of each injector remained virtually constant, independent of the injection pressure drop. For the bi-swirl coaxial injectors with the RN ≤ 1, the spray angles from the inner and outer swirl injectors exhibited differences of only a few degrees with respect to the value that was calculated using Eq. (8), and these are not dependent on the swirl direction. The spray angles of the inner liquid sheets in the case of the RN = 1 are similar to those of the case where the RN < 1. It is thought that the liquid sheet maintained its shape because the discharging of a portion of the sheet occurred without the occurrence of a collision with the outer injector nozzle. As the recess number increased above 1, however, the spray angle of the inner liquid sheet greatly decreased from approximately 64° to 14°. The measured spray angles in the co-swirl and counter-swirl coaxial injectors with the RN = 1.66 are similar to the predicted values according to Eq. (12). On the contrary, the measured spray angles of the co-swirl coaxial injector with the RN = 1.25 are approximately 10° greater than the predicted values. The spray image in Fig. 6 shows a heavy cloud surrounding the main liquid sheet. Here, the spray angle of the main liquid sheet is almost the same as

that of the bi-swirl coaxial injector with the RN = 1.66. Since there was insufficient length for the inner liquid sheet to become stable in the outer injector nozzle and the liquid sheet had a significant thickness, it is possible that the circumferential velocity of the sheet portion was greater than the main stream. Equation (12), however, could predict the spray angle of the inner liquid sheet in the bi-swirl coaxial injector with the RN > 1.

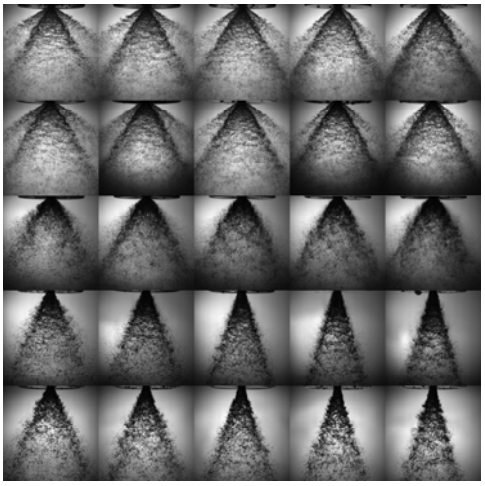

Fig. 8. Bi-injection spray patterns of the co-swirl coaxial injectors (from top to bottom: RN = 0.00, 0.53, 1.00, 1.25, and 1.66; from left to right: OD4, OD7, DP, OD5, and OD2 conditions).

4.2 Bi-Injection Spray Images and Spray Angles

Figure 8 shows the bi-injection spray patterns of the co-swirl coaxial injectors as a function of the recess length and the MR. The mixing conditions of the two liquids, such as the external, tip, and internal mixing, significantly affected the spray shape. For the co-swirl coaxial injectors with the RN < 1.00, the two liquid sheets were separately discharged and could be distinguished from each other. As the MR was increased, the outer liquid sheet contracted inward, but the inner liquid sheet remained unchanged. The spray images of the co-swirl coaxial injectors with the RN = 0.00 and 0.53 are similar. This finding means the recess length in those cases with the RN < 1.00 exerted a minor influence on the spray patterns. For the co-swirl coaxial injector with the RN = 1.00, it appears the two liquid sheets were combined and are difficult to distinguish. The combined liquid sheet shrank and appeared mist-like compared with the outer liquid sheet for the external-mixing injectors. For the co-swirl coaxial injectors with the RN > 1.00, the two liquids were perfectly combined inside the outer injector nozzle, and therefore one liquid sheet was discharged with a much reduced spray angle relative to the external-mixing inner/outer liquid sheets. As the MR was increased, the combined liquid sheet also became narrower. The spray images for the co-swirl coaxial injectors with the RN = 1.25 and 1.66 appear to be very similar.

To examine the effect of the swirl direction, the spray patterns of the bi-injection counter-swirl coaxial injectors are presented in Fig. 9 with varying recess lengths and MRs. The spray images of the counter-swirl coaxial injector with the RN = 0.00 are very similar to those of the co-swirl coaxial injectors with the RN = 0.00 and 0.53, as shown in Fig. 8. Although the spray angle is slightly reduced, the spray images of the counter-swirl coaxial injector with the RN = 1.00 are also similar to those of the co-swirl coaxial injector with the RN = 1.00. The spray images of the counter-swirl coaxial injector with the RN = 1.66, however, are very different from those of the co-swirl coaxial injectors with the RN = 1.25 and 1.66. As the MR was increased, the spray pattern significantly changed; the spray image in the vicinity of the MR = 2.50 looked like a liquid jet from a plain hole and it had lost its swirl motion. By gradually varying the MR, the swirl direction of the combined liquid sheet changed at around MR = 2.50, from clockwise (swirl direction of the outer liquid) to counter-clockwise (swirl direction of the inner liquid).

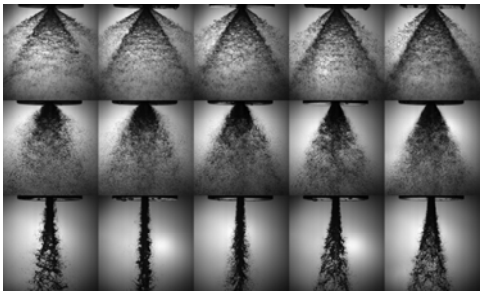

Fig. 9. Bi-injection spray patterns of the counter-swirl coaxial injectors (from top to bottom: RN = 0.00, 1.00, and 1.66; from left to right: OD4, OD7, DP, OD5, and OD2 conditions).

For the quantitative analysis, the spray angles of the bi-injection inner, outer, or combined liquid sheets were measured from the 100 photographs, and their averaged values are plotted in Figs. 10 and 11. Using the geometric dimensions of the present bi-swirl coaxial injectors and the measured inner/outer mass flow rates, the spray angles were calculated using the theoretical methods of Eqs. (8), (14), (19), and they are also shown in Figs. 10 and 11. Figure 10 shows the measured and calculated spray angles for the co-swirl and counter-swirl coaxial injectors with the RN < 1.00. From a comparison of Fig. 10 with Fig. 7, the spray angles of the bi-injection inner liquid sheets are only a few degrees greater than those of the single-injection inner liquid sheets, and they are almost constant, independent of the MR. On the contrary, the spray angles of the bi-injection outer liquid sheets are less than those of the single-injection outer liquid sheets, and they decreased with the increasing of the MR.

Several researchers (Bazarov *et al.* 2004; Long 2004; Kim 2007) used Eq. (14) to calculate the shape of the merged liquid sheet of the external-mixing bi-swirl coaxial injector. Kim (2007) reported that Eq. (14) could be applied to properly predict the combined liquid sheet shape. However, it should be noted that in these experiments, the swirl directions of the two liquid sheets are the same, and they merged into one liquid sheet outside of the injector. As the swirl direction between the inner and outer swirl injectors did not affect the spray angles, it is apparent that Eq.

(14) cannot be applied to the bi-swirl coaxial injectors in the case where the two liquid sheets are not mixed outside the injector. As noted by Bayvel and Orzechowski (1993), the liquid sheet entrains ambient gas. Chen and Yang (2014) noted the pressure difference across the liquid sheet that is due to the entrainment. Kim (2007) explained that the two liquid sheets approached one another due to the pressure decrease in the interspace between the two liquid sheets, and this was caused by the entrainment of the ambient gas. The studies of these researchers explain the present results. Since the inner mass flow rate is greater than the outer one, the entrainment by the inner liquid sheet is much greater than that by the outer one; thus, the spray angle of the outer liquid sheet approached more rapidly into the inner liquid sheet.

Figure 11 presents the measured and calculated spray angles for the co-swirl and counter-swirl coaxial injectors with the RN ≥ 1.00. In contrast to the results for the bi-swirl coaxial injectors with the RN < 1.00, the combined spray angles of the counter-swirl coaxial injectors are smaller than those of the co-swirl injectors. The measured spray angle of the co-swirl coaxial injector with the RN = 1.00 matched well with the value that was calculated using Eq. (14); however, the measured

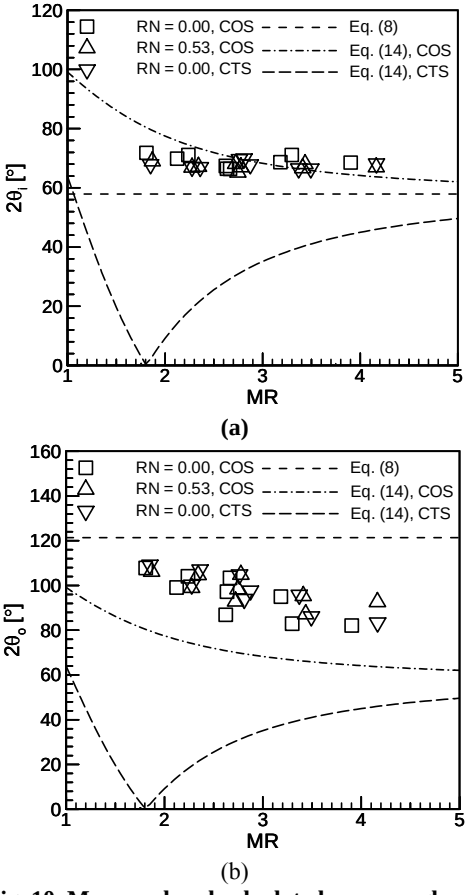

Fig. 10. Measured and calculated spray angles of the bi-injection inner/outer liquid sheets for the co-swirl and counter-swirl coaxial injectors with the RN < 1: inner swirl injectors (a) and outer swirl injectors (b).

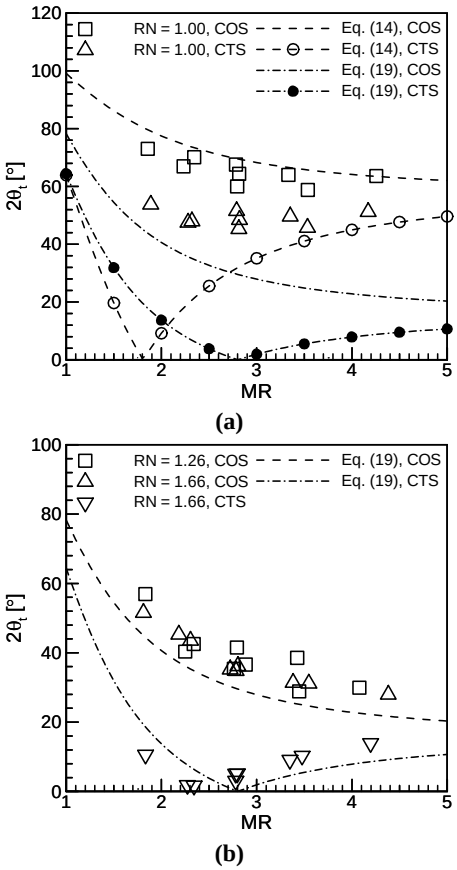

Fig. 11. Measured and calculated spray angles of the bi-injection combined liquid sheet for the co-swirl and counter-swirl coaxial injectors with the RN = 1 (a) and RN > 1 (b).

spray angle of the counter-swirl coaxial injector with the RN = 1.00 did not follow the value from Eq. (14), and it is almost constant in the present MR range. Though the two liquid sheets were partially mixed inside the injector, the measured spray angles exhibited larger differences from the values that were calculated using Eq. (19); this might be because the combined spray angles in the case of the RN = 1 were mainly measured using the unmixed portion of the outer liquid sheet. Irrespective of the swirl direction, however, Eq. (19) could accurately predict the spray angles of the combined liquid sheet of the internal-mixing bi-swirl coaxial injectors. Equation (19) could also approximate the swirl direction of the combined liquid sheet for the counter-swirl coaxial injectors.

5. CONCLUSION

Research on bi-swirl coaxial injectors was conducted to investigate the spray angle with respect to various parameters, such as the recess length, swirl direction, and mixture ratio. The single-injection and bi-injection spray angles were studied both experimentally and theoretically.

Regarding the single-injection inner and outer swirl injectors, it was confirmed that the spray cone angle is almost independent of the mass flow rate and the swirl direction. However, as the recess number of the bi-swirl coaxial injector increased beyond unity, the

spray angle of the liquid that was supplied by the inner swirl injector greatly decreased due to the collision on the wall of the outer injector. The variation could be accurately estimated from the suggested theoretical model, assuming the mass and momentum conservations.

Regarding the bi-injection bi-swirl coaxial injectors, the spray pattern and spray angle were significantly affected by the recess number and the MR. As the recess number was increased above 1.00, the spray angle drastically reduced; as the MR was increased, the spray angle of the outer liquid sheet or the combined liquid sheet generally decreased. For the bi-swirl coaxial injectors with the RN $\geq$ 1.00, the swirl direction greatly influenced the combined spray angle and the opposite swirl direction caused the combined spray angle to decrease. Further, the combined spray angle of the internal-mixing bi-swirl coaxial injector could be accurately predicted from the theoretical model suggestion that was derived using the mass/momentum conservation and the Skobelkin effect.

The present experimental and theoretical results can also be useful in bubble electrospinning.

ACKNOWLEDGEMENTS

This research is supported by the National Research Foundation (NRF-2013R1A5A1073861, NRF-2017R1A1A1A05001237, and NRF-2018M1A3A3A02065683) funded by the Ministry of Science and ICT, South Korea. The authors would like to thank the MSIT for its support.

REFERENCES

Abramovich, G. N. (1944). The theory of swirl atomizers. In *Industrial Aerodynamics*, Moscow, 114-121.

Ahn, K., Y. M. Han, S. Seo, and H. S. Choi (2011). Effects of injector recess and chamber pressure on combustion characteristics of liquid-liquid swirl coaxial injectors. *Combustion Science and Technology* 183(3), 252-270.

Ahn, K., Y. M. Han, and H. S. Choi (2012). Effects of recess length on discharge coefficients of swirl coaxial injectors. *Combustion Science and Technology* 184(3), 323-336.

Ahn, K., J. G. Kim, and H. S. Choi (2014). Effects of injector recess on heat flux in a combustion chamber with cooling channels. *Aerospace Science and Technology* 37, 110-116.

Ahn, K. and H. S. Choi (2017a). A study on discharge coefficients of closed-type swirl injectors for a liquid rocket engine. *Atomization and Sprays* 27(7), 569-578.

Ahn, K. and H. S. Choi (2017b). An extensive study on the discharge coefficients of open-type swirl injectors, *Atomization and Sprays* 27(10), 835-846.

Bayvel, L. and Z. Orzechowski (1993). *Liquid Atomization*. Taylor & Francis, Washington, D.C., U.S.A.

Bazarov, V., V. Yang, and P. Puri (2004). Design and dynamics of jet and swirl injectors. In V. Yang, M. Habiballah, J. Hulka, and M. Popp (Ed.), *Liquid Rocket Thrust Chambers: Aspects of Modeling, Analysis, and Design*, Reston, Virginia, U.S.A., 19-103.

Borodin, V. A., Y. F. Dityakin, L. A. Klyachko, and V. I. Tagodkin (2004). *Atomization of Liquids*. Air Force Foreign Technology Division Rep. FTD-MT-24-97-68, U.S.A.

Chen, X. and V. Yang (2014). Effect of ambient pressure on liquid swirl injector flow dynamics. *Physics of Fluids* 26(10), 102104.

Fu, Q., L. Yang, and X. Wang (2010). Theoretical and experimental study of the dynamics of a liquid swirl injector. *Journal of Propulsion and Power* 26(1), 94-101.

Fu, Q., L. Yang, and X. Wang (2011a), Geometrical effects on the fluid dynamics of an open-end swirl injector. *Journal of Propulsion and Power* 27(5), 929-936.

Fu, Q., L. Yang, and Y. Qu (2011b). Measurement of annular liquid film thickness in an open-end swirl injector. *Aerospace Science and Technology* 15(2), 117-124.

Fu, Q., L. Yang, W. Zhang, and K. Cui (2012). Spray characteristics of an open-end swirl injector. *Atomization and Sprays* 22(5), 431-445.

Gill, G. S. and W. H. Nurick (1976) *Liquid Rocket Engine Injectors*. NASA Rep. SP-8089, U.S.A.

Jeon, J., M. Hong, Y. M. Han, and S. Y. Lee (2011). Experimental study on spray characteristics of gas-centered swirl coaxial injectors. *Journal of Fluids Engineering* 133(12), pp. 121303.

Khavkin, Y. I. (2004). *The Theory and Practice of Swirl Atomizers*. Taylor & Francis, New York, U.S.A.

Kim, D. (2007). *Spray Characteristics of Swirl Coaxial Type Injectors for Liquid Rocket Engines*. Ph. D. thesis, Seoul National University, Seoul, Korea.

Kim, S. (2011). *Internal Flow Characteristics of Swirl Type Injectors for Liquid Rocket Engines*. Ph. D. thesis, Seoul National University, Seoul, Korea.

Kim, J. K. (2013). *Spray Structures in High Pressure Environment of Gas-centered Swirl Coaxial Injector for Staged Combustion Cycle Engines*. Ph. D. thesis, Seoul National University, Seoul, Korea.

Kim, T. H., N. C. Cho, and Y. T. Keum (2003). A study on performance of dual swirl injector with different recess length, *Journal of the Korean Society of Propulsion Engineers* 7(2), 62-69.

Long, M. R. (2004). *Swirl Injectors for Oxidizer-Rich Staged Combustion Cycle Engines and Hypergolic Propellants*. Ph. D. thesis, Purdue University, U.S.A.

Sivakumar, D. and B. N. Raghunandan (1998). Role of geometric parameters on the drop size characteristics of liquid–liquid coaxial swirl atomizers. *Atomization and Sprays* 8(5), 547-563.

Sivakumar, D. and B. N. Raghunandan (2003). Formation and separation of merged liquid sheets developed from the mixing of coaxial swirling liquid sheets. *Physics of Fluids* 15(11), 3443-3451.

Vijay, G. A., N. S. V. Moorthi, and A. Manivannan (2015). Internal and external flow characteristics of swirl atomizers: a review. *Atomization and Sprays* 25(2), 153-188.

Yang, L., M. Ge, M. Zhang, Q. Fu, and G. Cai (2008). Spray characteristics of a recessed gas-liquid coaxial swirl injector. *Journal of Propulsion and Power* 24(6), 1332-1339.

Yoon, W. and K. Ahn (2017). Flow characteristics of close-type swirl injectors manufactured by a 3D printer. *Atomization and Sprays* 27(2), 131-137.